1-1-2007

Three-dimensional modelling of ground surfaces

Ming Li
Ryerson University

THREE-DIMENSIONAL MODELLING OF GROUND SURFACES

by

Ming Li

B.Eng, Beijing University of Aeronautics and Astronautics

Beijing, China, 1997

A Thesis

presented to Ryerson University

in partial fulfillment of the

requirements for the degree of

Master of Applied Science

in the program of

Mechanical Engineering

Toronto, Ontario, Canada, 2007

I hereby declare that I am the sole author of this thesis.

I authorize Ryerson University to lend this thesis to other institutions or individuals for the purpose of scholarly research.

I further authorize Ryerson University to reproduce this thesis by photocopying or by other means, in total or in part, at the request of other institutions or individuals for the purpose of scholarly research.

Ryerson University requires the signatures of all persons using or photocopying this thesis.

Please sign below, and give address and date.

Three-dimensional Modelling of Ground Surfaces

A thesis for the degree of

Master of Applied Science, 2007

by

Ming Li

Department of Mechanical Engineering

Ryerson University

Abstract

The efficiency and quality of abrasive machining processes influence costs and quality of elements produced, as well as whole products. Hence, the estimation of surface characteristics can greatly facilitate the requirements of performance evaluation. But the surface finish is dominated by many factors and a physical model which could predict it is not practical. Therefore, it is very important to develop modelling techniques for the reliable prediction of surface characteristics.

This thesis describes the development of a three-dimensional predictive modelling methodology for surface characteristics of a ground surface. The methodology uses solid modelers to generate the chips and remove them from the solid model of the workpiece. This

results in a surface model which represents the ground surface in three dimensions. Various surface characteristics can then be deducted from this model.

The modelling of individual abrasive grains follows a statistical distribution which depends on the grinding tool characteristics. The cutting path depends on the relative motion between the tool and workpiece.

The methodology was implemented for three different types of tool path. The results are in agreement with expected values.

Acknowledgements

I am very grateful to Dr. Ahmad Ghasempoor and Dr. Jeff Xi for giving me the opportunity to work on such an exciting project and for their constant encouragement and valuable guidance throughout this study. Thanks to Dr. Ahmad Ghasempoor and Dr. Jeff Xi for the help and offering me flexible working hours. Thanks to my wife for the patience and great support during the time I worked on the thesis.

This work is funded by the National Science and Engineering Research Council of Canada.

Table of Contents

List of Tables

List of Figures

Nomenclature

a:	Constant number
B:	Width of the grinding zone
D:	Wheel diameter
D_{gmax} :	Largest dimensions of the grains
D_{gavg} :	Average grain dimension
Ds:	Mean value of the wheel diameters
M:	Grit size
r:	Grit distance from the grinding tool center
R_a:	Average surface roughness
S:	Structure number
t:	Time
V_g:	The density of the wheel
V_s:	Feed speed
V_θ :	Wheel speed
V_w:	Wheel wear
W:	Width of the grinding tool
X:	x coordinate of the grit path
Y:	y coordinate of the grit path
z:	Truncated value

μ :	Mean value
μ_w:	Mean value of the protrusion height
σ :	Stand deviation
Δ :	Grain interval
Δr_s:	Measured decreased wheel radius

Chapter 1. Introduction

1.1. Grinding Process

Although grinding is probably one of the oldest manufacturing processes, it still persists as an important component of modern manufacturing. Grinding is a finishing process with a low material removal rate, which is best suited for producing parts of high precision and surface quality. This has made the grinding process the subject of extensive research.

All grinding processes use many cutting edges, randomly located, to remove material. The chips formed in grinding are very small relative to turning or milling operations. These small chips are one of the reasons that grinding can maintain generally superior surface finishes and closer tolerances than other chip making processes. In order to produce ground parts that have desirable surface properties, it is necessary to understand the surface generation mechanisms involved in the grinding process.

Surface grinding is a manufacturing process during which a grinding wheel contacts the workpiece surface and removes a minute amount of material, such that a flat surface is created. The term "surface grinding" designates any process which accurately processes or grinds a surface [1].

Parts may require surface grinding for several reasons. The following are a few of the more common reasons:

- Produce a very flat surface.
- Very accurate thickness tolerance specified.
- A very smooth surface roughness is specified or required.

Surface grinding machines and processes were developed to manufacture very tight tolerances, smooth surface finishes, and removing material from very hard materials.

1.2. **Research Objectives**

Grinding is widely used for final machining of components requiring smooth surfaces and precise tolerances. Extensive research conducted during the past 40 years has provided a relatively clear understanding of many diverse aspects of the grinding process. Grinding is a very complex process in that it involves many physical phenomena and numerous stochastic factors. Therefore, it is more economical to model the grinding process without the grinding experiments which cost more labor and time. The objective of this work is to use the understanding of the grinding process to predict the surface finish of a ground surface in a surface grinding operation. Most of the previous research in this area has been limited to cylindrical grinding. Surface grinding poses a more challenging problem since the movement of individual grit follows a very complicated path. In this thesis, a three

dimensional solid modeling method is used to generate the predictive model. The goal is to provide a robust methodology that can be used with any tool path in surface grinding.

The thesis is organized as follows:

Chapter 1 is a brief introduction of the grinding process and thesis outline.

Chapter 2 reviews the background and presents an overview of the related research literature.

Chapter 3 presents the material removal mechanisms and set-theoric modeling of ground surface, modelling of grits and path and the wear of the grinding wheel.

Chapter 4 presents the modelling results for five different case studies.

Chapter 5 discusses the modelling results.

Chapter 6 contains the conclusions and recommendations for future work.

Chapter 2. Literature Review

2.1. Types of Grinding Processes

Grinding is a machining process that employs an abrasive grinding wheel rotating at high speed to remove material from a softer material. Four basic grinding processes are illustrated in Fig. 2.1. Face grinding is grinding using the face of a grinding wheel which can be contrasted with peripheral grinding in which grinding is performed predominantly with the peripheral surface of the grinding wheel. Surface grinding usually refers to grinding flat or profiled surfaces with a linear motion while cylindrical grinding refers to the grinding of a rotating workpiece. Cylindrical grinding may be performed internally or externally.

Surface grinding methods include: horizontal-spindle, vertical-spindle, vertical-spindle rotary grinding, horizontal spindle single disk, and vertical swivel head grinding as listed in Fig. 2.1.

According to the requirement of the final surface, the grinding processes are classified into two groups: coarse grinding and fine grinding. While grinding of metallic material still constitutes a major portion of grinding applications, the other areas of application have gained importance. Silicon wafer grinding is an important step in semiconductor processing for thinner and therefore smaller integrated circuits (IC). Semiconductor wafers are thinned to aid the sawing operation and lower thermal resistance.

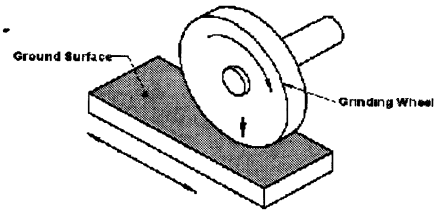

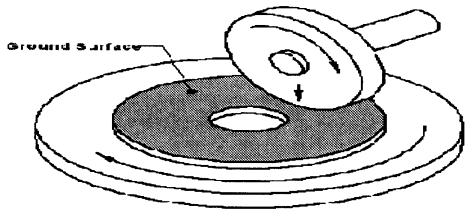

Horizontal spindle reciprocating table surface grinding	Horizontal spindle rotary table surface grinding

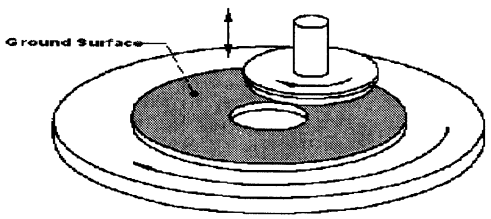

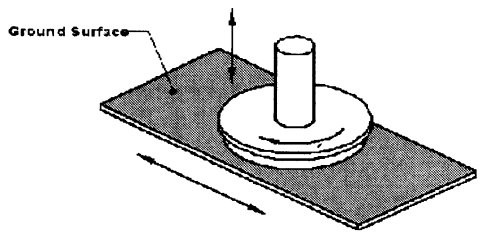

Vertical spindle rotary table surface grinding	Vertical spindle reciprocating table surface grinding

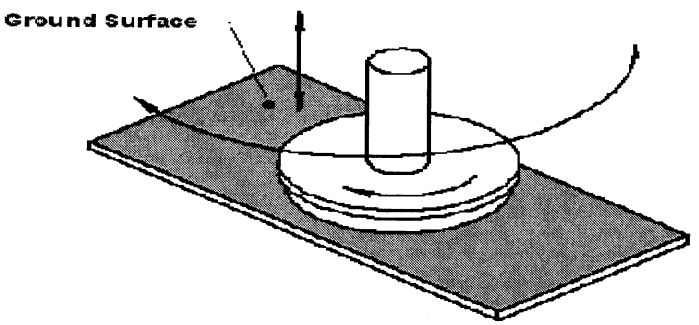

Vertical spindle swivel head surface grinding

Figure 2.1: Surface grinding methods [1]

2.2. Grinding Process

2.2.1. Grinding Wheel

The abrasive type, abrasive grit size, hardness grade, grain structure and bond type all influence grinding wheel performance. Changes in the amount and type of each of these elements will affect the performance of the wheel. Here are brief descriptions of the important factors in a grinding wheel [2].

2.2.1.1. Abrasive Type

The abrasive grain is what actually removes material from the piece. There are four basic abrasive types:

- Aluminum Oxide (high speed steel applications)
- Silicon Carbide (carbide grinding applications)
- Diamond (carbide grinding applications)
- Cubic Boron Nitride (CBN) (high speed steel applications)

Grit type is generally aluminum oxide, silicon carbide, ceramic or any combination of these. Aluminum oxide is by far the most popular. Silicon Carbide grits are commonly either black or green. Black silicon carbide is used to grind non-ferrous metals, such as aluminum and brass and also plastics, rubber, and stone products, such as marble and granite. Black silicon carbide is a very sharp grit. Green silicon carbide is an even sharper

grit than black and is used primarily for carbides, titanium and plasma sprayed materials. On steels, silicon carbide is used as a polishing/finishing grit. Manufacturers will often blend a small percentage of silicon carbide in with aluminum oxide grit in grinding wheels and honing stones to achieve a better workpiece surface finish on steels.

2.2.1.2. Abrasive Grit Size

Abrasive grains are sized according to an established worldwide standard and are designated by a numerical grit size. Grit size typically runs from coarse (16 -24 grit), medium (36 - 60 grit) and fine (80-120 grit). Superfine grits run from 150 and higher. Grinding wheels usually will be between 24 and 100 grits. Honing stones and jointing stones and other polishing abrasives will be 150 grit and higher. A large grit number represents a tool with small grit size. Coarse grain size (a smaller number) will increase stock removal rate, but provide less surface finish quality. Fine grit sizes (larger numbers) provide less stock removal, but improve surface quality [2].

2.2.1.3. Hardness Grade

Hardness is rated from A-Z with 'A' being the weakest bond and 'Z' being the strongest. This grade represents the amount of bond used in the wheel. Generally, harder grades produce a better finish, but will have a tendency to load up faster than softer grades. A weak bond is preferred for grinding harder materials while a stronger bond is desired for

softer materials. A typical weak bond for steel would be in the 'F, G or H' range. A medium hardness would be in the 'I, J or K' range and stronger bonds in the 'L, M, or O' range. Selection of the hardness is dependent on the grit type, the material being ground, the amount of stock removed, and a number of other factors.

2.2.1.4. Grain Structure

Structure is the spacing between abrasive grains. The structure depends on a variety of factors, especially how difficult the material is to grind. In general, a closer spacing would make a tougher wheel. Grinding wheel engineers will typically adjust the bond strength depending on the application. An open structure wheel will be very aggressive, but will not hold its form as well and wear out faster.

A denser wheel will generally provide a better finish, but will generate more heat and slower metal removal. Wheel structure is also critical in making a finish wheel with smaller dimension in order to grind tight corners or small radii [2].

2.2.1.5. Bond Type

The grinding wheel bond (the binding agent), is the material which holds the abrasive grains together. Without the right bond, the grinding wheel will disintegrate at high speeds. Four major types of bond are: Vitrified (V), Retinoid (B), Rubber (R), and Metal (M). There are a multitude of variations in each category that manufacturers use to fine tune grinding wheel

specifications to improve performance.

2.2.2. Workpiece

Workpiece characteristics that affect the surface finish in grinding include the material's mechanical properties, its machinability, thermal stability, abrasion resistance, its microstructure and chemical properties. Geometry is another workpiece factor for grinding, determining how well the grinding wheel and workpiece conform to each other. Workpiece geometry can restrict coolant flow to the work zone. Sharp edges or very tight radii are special considerations that should be included in the analysis of the workpiece. Part quality requirements are critical factors to the successful grinding operation. These include feature tolerances and surface finish requirements.

2.2.2.1. Wheel Selection Factors

Obviously, selecting the abrasive is an important factor in grinding. Grain types, properties, size, distribution and concentration need to be identified. The tool holder for these grains (bond) is an equally important factor. Bond characteristics can be classified by their type, hardness, stiffness, porosity and thermal conductivity. How the grinding wheel is constructed influences the cut. Shape and size of the wheel should be matched to the workpiece geometry. Core material of the wheel and its form or profile need to be compatible with the other selected factors.

A diamond wheel is specifically used for carbides, plastics and other synthetic materials. It will not grind steel well. CBN wheels should only be used on steels. There is a hybrid grit available that will grind both. However, it is a compromise in wheel life and grind-ability.

2.2.3. Grinding Parameters

Many factors affect surface roughness in grinding. Some of the more important ones are: cutting speed, feed speed, depth of cut, material characteristics, wheel loading and dressing, coolant types, machine stiffness and age, surface conditions, centre conditions and vibration of the wheel.

Saglam et al. [3] presented an experimental study on the effects of grinding parameters on roundness and surface roughness using orthogonal arrays developed by Taguchi. The surface roughness was found to be controlled mainly by work speed and depth of cut unless the feed rate was increased to an excessive level. The improvement in the surface finish was seen at low work speeds, small depths of cut, higher cutting speeds and also lower feed rates. Chip thickness could be reduced by decreased work speeds in cylindrical grinding. As a result, the cutting parameters that influence roundness error and surface roughness quality must be kept under control in order to increase part quality.

Kopac et al. [4] provided a review of state of the art technology of high-performance grinding at increased wheel speeds with highly efficient abrasives. They emphasized that an

increased grinding speed is the most important factor in achieving improved quality, tool life and productivity. If cutting speed and material removal rate are increased while maintaining constant chip thickness, as shown in Fig. 2.2, the result is constant grinding forces, wheel wear and workpiece surface roughness. On the other hand, the increase in the cutting speed at constant material removal rate, as shown in Fig.2.3, results in the reduction in grinding forces, wheel wear, workpiece surface roughness and size/form accuracy error.

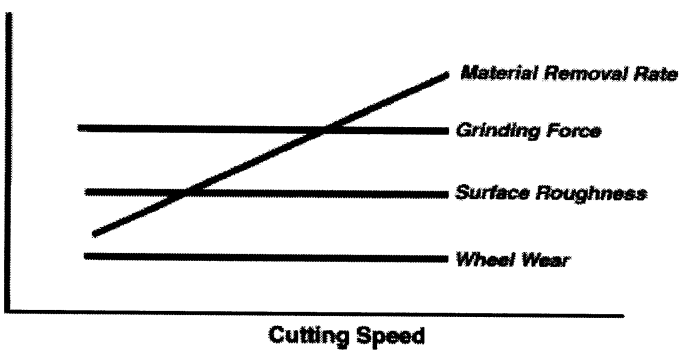

Figure 2.2: High-performance HSG at constant chip thickness [4]

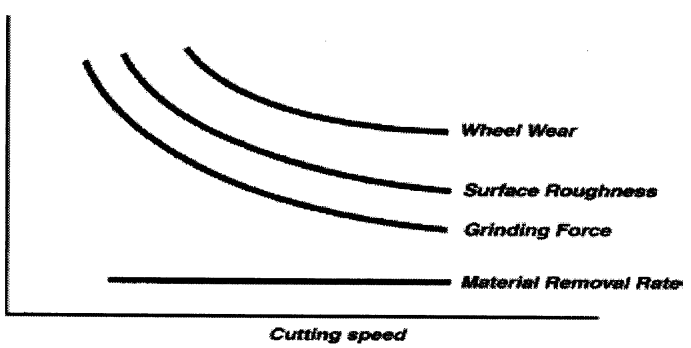

Figure 2.3: High-quality HSG at constant material removal rate [4]

To achieve maximum influence on the grinding process, it is more effective to deal with the grinding process as a whole. P. Asokan et al. [5] optimized the grinding process parameters such as wheel speed, workpiece speed, depth of dressing, and lead of dressing by minimizing production cost and maximizing production rate as well as the finest possible surface finish.

2.3. Predictive Modelling of Surface Finish

Successful grinding requires a continuous effort to produce improvements in several key areas. Some of this deal with the technology of grinding a good part and others cover the economics of producing a part profitably. Technology results include meeting or exceeding the specifications required for the finished workpiece. In order to estimate the final surface roughness, many researchers have developed models to simulate the grinding process.

The most direct way of simulating a grinding wheel surface is measuring and using the grinding wheel topography directly in the simulation [6]. But measuring the whole grinding wheel is a time-consuming activity since a realistic simulation of the grinding process requires a vast amount of wheel surface. As an alternative, an empirical model developed by Suto and Sata [7] relates surface finish to the number of active cutting edges using the experimental data, and it has been found that there is a logarithmic relationship between them. Chen and Rowe [8] developed a topography model that assumed uniform, spherical grains randomly arranged in the bond material, and that were subsequently dressed. A

representative section of the wheel is modeled by uniformly arranging the grains in the bond material, randomizing their location, and subsequently performing a dressing operation.

Agarwal et al. [9] adopted a new surface roughness prediction model for ceramic grinding. This model shows a proportional relationship between the surface roughness and the chip thickness expected value under the assumption that the profile of the groove generated by an individual grain to be semi-circular in shape. They also developed a new analytical model for the prediction of arithmetic mean surface roughness based on the stochastic nature of the grinding process. A simple relationship between the surface roughness and the chip thickness was obtained, which was validated by experimental results of silicon carbide grinding.

Zhou and Xi [10] developed a new method to predict the surface roughness of the workpiece for the grinding process. It takes into consideration the random distribution of the grain protrusion heights. A search method is developed to systematically determine the surface profile from the highest protruded grain in a descending order. Fig. 2.4 shows an example of simulated wheel topography.

Torrance and Badger [11] developed a grinding wheel topography model that incorporates not only stochastic quantities but also the dressing of the wheel surface. The basic premise of the model is that uniform, spherical grains are distributed randomly in the bond material.

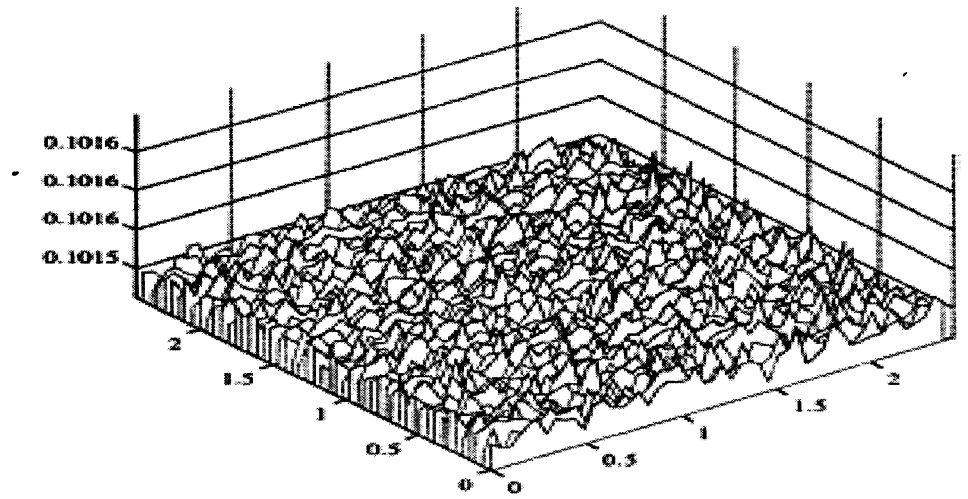

Figure 2.4: Simulated wheel topography [10]

Nguyen and Butler [12] took into consideration the wheel-workpiece interaction and an algorithm was proposed to identify the active abrasive grains and their attack angles from the wheel topography. Based on the critical values of the attack angle, the abrasive grain is determined to cut, plough or rub the workpiece.

Rogelio et al. [13] presented a model to predict the arithmetic mean surface roughness directly from the estimated chip thickness probability density function developed. The expected close relation between the surface roughness and the chip thickness is analytically justified based on a probabilistic analysis, where the main random variable is the chip thickness as shown in Fig. 2.5. The simple relationship found is based on the stochastic nature of the grinding process that allows for a time efficient solution. The model expresses the ground finish as a function of the wheel microstructure, process kinematics conditions

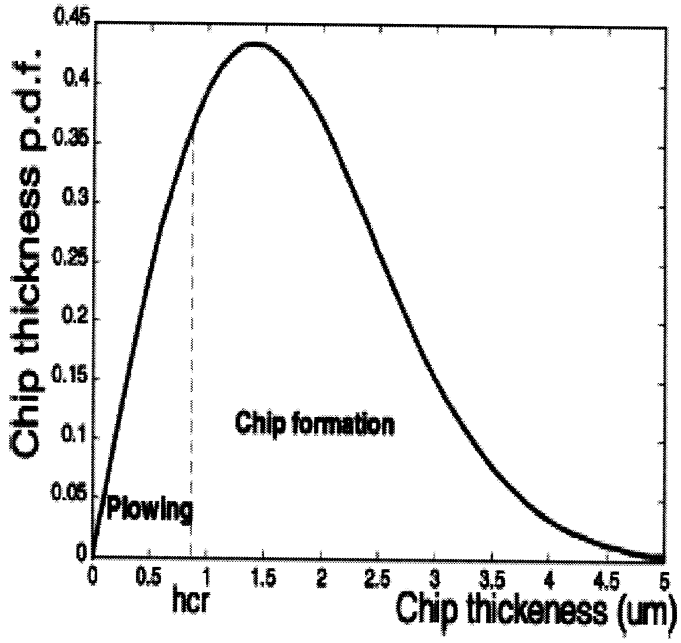

Figure 2.5: Chip thickness probability density function [13]

and the material properties. The analysis includes a geometrical analysis of the grooves left on the surface by ideal conic grains. The material properties and the wheel microstructure are considered in the surface roughness prediction through the chip thickness model. A simple expression that related the surface roughness to the chip thickness was found.

Hongqi et al. [14] presented a dynamic/chatter model for cylindrical plunge grinding processes through a time domain simulation approach. The procedure to simulate the grinding processes has been presented along with simulated results of external plunge grinding as a function of operating parameters. Although the simulations and validations

were carried out using example cases of external plunge grinding, it is claimed that the model is valid for both external and internal plunge grinding.

Murad et al. [15] designed an adaptive neuro-fuzzy system to predict the surface roughness, on-line, during the grinding process. The power spectral density parameters were used as inputs to the system to predict roughness on-line. The neural nets and fuzzy logic approaches have the inherent shortcomings that these systems need to be retrained for different process parameters (i.e., rigidity of the robot's end effectors, accelerometer's location, workpiece material, and pneumatic system's parameters). Another limitation of this approach is that the numerical values of fuzzy membership functions and neural nets structure would not probably be optimal for another surface finishing or manufacturing process. This may necessitate further re-training.

2.4. **Summary**

All the research discussed above deals with peripheral grinding where the outside of the grinding wheel is used. However, there are many grinding applications where the face of the grinding wheel is used. Examples include surface grinding and polishing applications. Surface grinding is more difficult to model because of the more complex path traversed by each grit. An example is shown in Fig.2.6 [16]. In this application, silicon wafers are ground to remove waviness and improve surface finish. The path of each grit is a combination of two rotary motions. This thesis presents a new predictive model of surface finish for

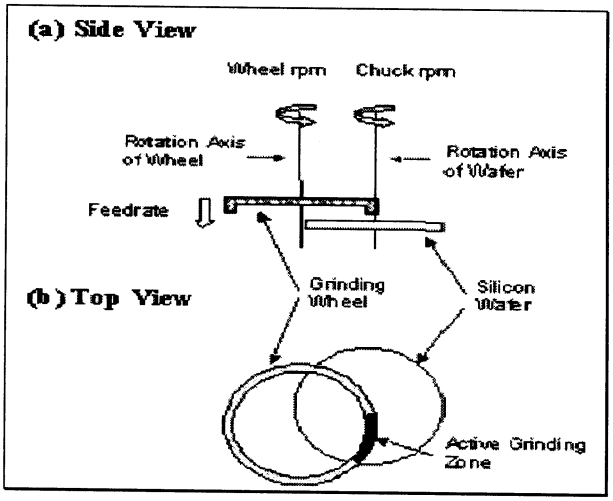

Figure 2.6: Illustration of wafer grinding [16]

peripheral grinding processes which can be easily applied to this type of application.

Another shortcoming in the methods reported in the literature is the treatment of the grinding process as a two-dimensional process. A three-dimensional model is one where not only are the grains considered as three-dimensional objects, but a 3D surface is produced to estimate a measured topography [17]. In this Thesis, a 3D modelling has been developed to evaluate the arithmetic mean surface roughness from the chip thickness probability density function, and the relationship between surface roughness and the chip thickness has been established with the chip thickness as a random variable. This model approximates the grinding wheel topography by a randomized arrangement of three dimensional triangular grains and a 3D surface is formed according to the kinematics of the grinding tool and workpiece.

2.5. Effect of Wheel Worn on Surface Finish

The main mechanisms of wheel wear are: attritious wear, grain fracture, and bond fracture [18]. Attritious wear involves dulling of abrasive grains and the growth of wear flats by rubbing against the workpiece. Grain fracture refers to removal of abrasive fragments through fracture within the grain, and bond fracture occurs by dislodging the abrasive from the binder. Another type of wear is binder erosion, which is likely to reduce the bond strength and promote grain dislodgement, especially with resin and metal-bonded wheels [5]. The relative contribution of each of the three causes of wear mechanisms can be estimated from the wear particle-size distribution together with measurements of wear-flat area and volumetric wear. Research has shown that attritious wear is negligible and the most of the wear is due to the grain fracture. The grain fracture factor is more prominent as the wheel hardness increases because of the greater bond strength allied with the greater probability of the abrasive grain undergoing fracture prior to being finally dislodged. Without a method to make the tool surface sharper the abrasive grains would become extremely dull, therefore causing large grinding forces and thermal damage to the workpiece [18]. The model developed in this thesis will take into account the wheel wear by incorporating the statistical changes in the grain distribution.

Chapter 3. Methodology

3.1. Introduction

Grinding technology has improved considerably in recent years in terms of productivity and precision. Modern grinding wheels with enhanced wear resistant abrasives and improved bond systems have all contributed to this. A predictive model which can estimate the surface finish without laborious experiments would be very useful in reducing the cost of products.

This chapter will introduce the methodology used in developing such a model including material removal mechanisms, grinding process modelling, grits formation, grits path, grit wear and surface roughness calculations.

3.2. Material Removal Mechanism

The removal process during the engagement of an abrasive cutting edge on the surface of a workpiece mainly depends on the prosperities between the active surfaces. A basic distinction can be made among three different mechanisms: micro plowing, micro chipping and micro breaking [18].

In micro plowing, there is a continual plastic material deformation with negligible material loss. In practice, the simultaneous impact of several abrasive particles or the repeated impact of one abrasive particle leads to material failure at the border of the cutting paths. Ideal

micro chipping provokes chip formation where the chip volume equals the volume of the evolving grits cutting the workpiece. Micro plowing and micro chipping mainly occur during the machining of ductile materials. The proportion of micro plowing versus micro cutting depends on the prevailing conditions such as the matching of the active grits, grinding parameters and cutting edge geometry [18].

Micro breaking occurs in case of crack formation and spreading. The volume of a chip removed can be several times larger than the volume of the cutting groove. Micro breaking mostly occurs during the machining of brittle materials such as glass, ceramics, and silicon.

In this thesis, the micro chipping will be considered to be the dominant process and other mechanisms will be neglected, effectively limiting the scope to ductile engineering material.

3.3. **Grinding Process Modelling**

Knowledge of the basic principle of a manufacturing process is a prerequisite for its effective improvement and optimization. In the case of the grinding process, the investigation of the chip removal mechanisms is complicated due to many factors. The first problem is the characterization of the tool. The abrasive grains are three-dimensional and statistically distributed in the volume of the grinding wheel. The geometry of a single cutting edge is also complex. Moreover, there is a near simultaneous engagement of the cutting edges involved in the process. The surface formation is the sum of these interdependent cutting edge

engagements, which are distributed stochastically. Furthermore, the chip formation during grinding takes place within a range of a few microns. The small chip sizes make the observation even more difficult.

3.3.1. Grinding Wheel Topography

The cutting process in grinding is the sum of individual, microscopic cutting processes, whose temporal and local superposition leads to a macroscopic material removal. As a consequence, the cause-and-effect principle of grinding can only be described on the basis of the cutting behavior of the individual abrasive grains. The most important parameter is the number of engaged cutting edges. An exact determination of the geometrical engagement conditions of the single cutting edges, however, is not possible for manufacturing processes like grinding. Due to the stochastic distribution of the geometrically undefined cutting edges, their position and shape cannot be exactly determined. Therefore, the position, number, and shape of the abrasive grains are analyzed statistically and related to the process kinematics and geometry to achieve a specification of the engagement conditions of the abrasive grain. Thus, grinding results can be related to events at the effective area of grinding contact for particular input values of machine and workpiece parameters and the theoretical chip thickness, length, and engagement angle. Knowing the overall relations between input values, cutting and chip values, as well as process output values, the behavior of the process can be cohesively described and used to improve the set-up of the machining process. This

implies a wheel specification suitable for the grinding situation and the choice of parameters leading to an economical grinding process.

The methods of determining the grinding wheel topography can be divided into static, dynamic and kinematic methods.

In the static method, all abrasive grains on the surface of the grinding tool are considered. The kinematics of the grinding process is not taken into account.

In the dynamic method, the number of actual abrasive grain engagements is measured. The active cutting edge number is the sum of cutting edges involved in the cutting process.

The kinematic method combines the effects of the kinematics of the process with the statistically determined grain distribution for the specification of micro-kinematics at the single grain level [18].

In this thesis, a variation of the kinematic method is used to develop a predictive model of surface finish in grinding.

3.3.2. Active Cutting Edge

The microstructure of the grinding wheel is composed of numerous individual abrasive grains which are stochastically distributed. All grains are potential cutting points; however, only some of grains are actually engaged in the cutting operation, these are called active

cutting edges or grains. The active cutting edges are responsible for the generation of the ground surface.

The number of cutting edges per unit length and their orientation are characteristic quantities of a grinding wheel. One grain may have one or more cutting edges; however, it is sufficient to consider the cutting edges that belong to the same grain as one cutting edge [19]. The density of cutting edges and the stiffness of contact are closely related to each other. The density of cutting edges increases with grain size if the grade is the same. With the same grain size, the density of cutting edges increases with grade [20].

The active cutting edges cut grooves from the workpiece surface. If all the active cutting edges were of the same protrusion heights, the cutting path generated would consists of successive identical scallops [10]. On the other hand, when cutting edges have different protrusion heights, the longer protrusion grains would generate deeper grooves on the workpiece surface than shorter ones. The cutting path generated would then depend on the engagement of the outmost protruded grains. A predictive model of the grinding process must take into account the random protrusion heights of a typical grinding wheel.

Since the cutting edges on the wheel are randomly distributed and many cutting edges contribute to generate the machined surface, a statistical analysis of the distribution and quantity of cutting edges is conducted to describe the necessary configuration of the wheel

surface in a deterministic way. While there are some examples of this method of modelling for grinding using the periphery of grinding wheels, processes using the surface of grinding wheels have not been successfully modeled. This thesis introduces a versatile method for predictive modelling of a ground surface using three dimensional solid modelling and Boolean operations. The method is well suited to operations where the cutting grains follow complicated paths.

3.4. Set-theoric Modelling of Ground Surfaces

The methodology used in this work uses grinding process parameters to generate solid models of individual chips. These chips are then removed from a given workpiece to generate a three-dimensional surface topography from which all surface characterization information can be deducted. The commercial solid modeler used in this thesis is essentially a collection of computer algorithms for representing solid objects. These algorithms can be used to generate different solid models, add or subtract them from other solid models, etc. Existing grinding modelling methods for cylindrical grinding rely extensively on analytical equations. The Modelling of a surface requires keeping track of active grains [21]. While this method is useful when the cutting path of grits is simple, complicated grit paths will make the method virtually intractable.

The 3D solid model technique developed in this thesis closely mimics the manufacturing process by performing Boolean subtraction operations corresponding to the grinding steps

preserving the order in which these steps are performed. An example is shown in Fig. 3.1. First a workpiece is generated using a solid modeler (Fig.3.1a). A grit section is then formed according to the wheel parameters (Fig.3.1b). The grinding path is then obtained according to the kinematics of the grinding process including wheel and work speed (Fig.3.1c). The chip can then be subtracted from the workpiece (Fig.3.1d), to represent the actual chip removal. The final surface is achieved by repeating, in a statistical sense, this process for the entire grinding process. For the surface finish to be predicted accurately, the cutting grits, their distribution and cutting path must be modelled accurately. The following sections discus, in detail, the parameters and methods used to develop the model.

3.5. Modelling of Grits

Grinding wheels contain hard abrasive grains embedded in the bond bridges. The grains, randomly distributed on the wheel surface, differ in terms of size, shape, orientation, and distribution density over the wheel surface, thereby resulting in random variations in the protrusion heights from the wheel surface [10].

Grit number is defined in terms of grain sizes. The surface roughness is most sensitive to the abrasive grit size. An increase in abrasive grit size results in a rougher surface [22]. The protrusion height of cutting grains can be obtained based on the average grit size and its standard deviation. Since each nominal grit size includes a range of abrasive particle sizes,

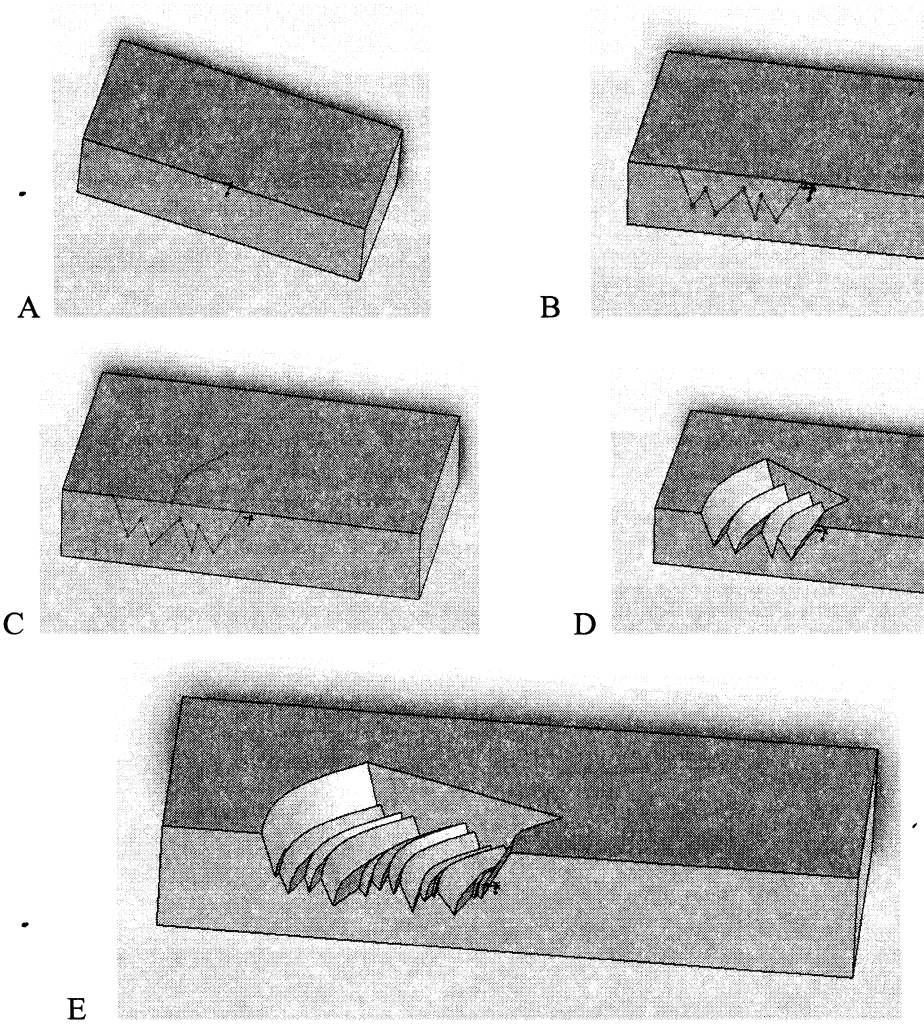

Figure 3.1: Set-theoric modelling of chip removal

the grit dimension corresponding to a particular grit number might be characterized by an average value [10]. However, the grit dimension $d_{g\max}$ is often quoted either as equal to the aperture opening of the control sieve, or alternatively according to the relationship [5]:

$$d_{g\max}(mm) = 15.2M^{-1} \tag{1.1}$$

Where M is the grit number.

Eq.(3.1) approximates the grit dimension as 60% of the average spacing between adjacent wires in a sieve whose mesh number equals the grit number M. The abrasive grain dimensions according to both of those methods are plotted in Fig. 3.2 as a function of grit number. Within a range of abrasive particle sizes, the above dimension could be regarded as the largest dimension of the grains. The average grain dimension can be approximated as [5]:

$$d_{gavg}(mm) = 68M^{-1.4} \tag{1.2}$$

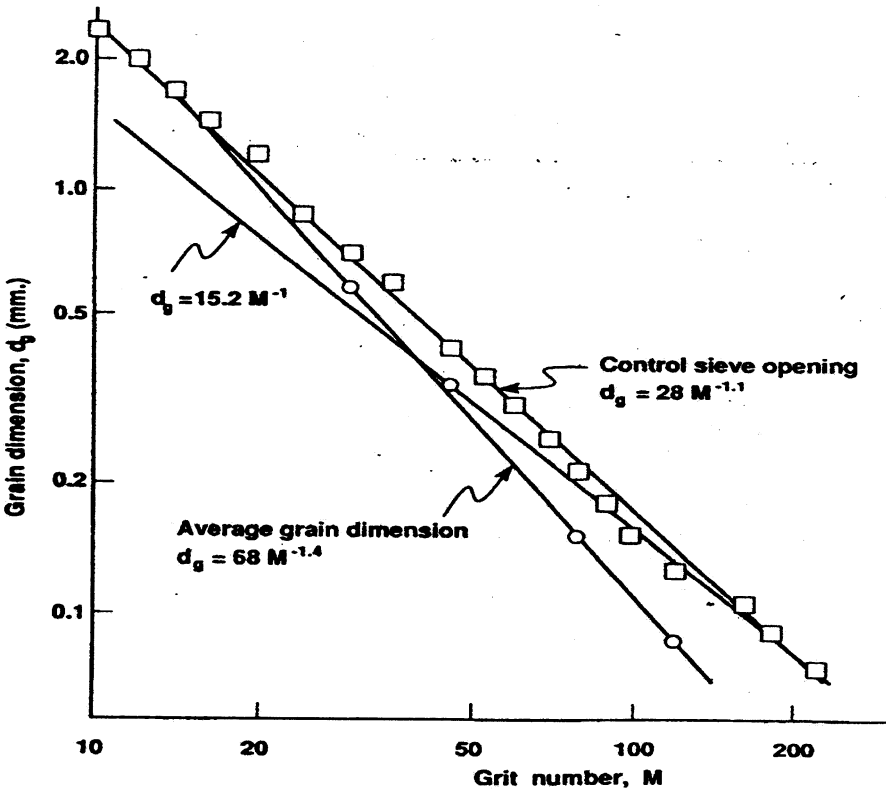

Figure 3.2: Grain dimension versus grit-number based on sieve wire spacing, control sieve opening and grain dimension [21]

The grain protrusion height is found by using the Gaussian distribution for a given mean value

and standard deviation [10]. For a given grit number, the former can be determined by:

$$\mu = d_{gavg}(mm) \tag{1.3}$$

And the standard deviation can be estimated as:

$$\sigma = (d_{g\max} - d_{gavg})/3 \tag{1.4}$$

In order to form the final wheel topology, the grain interval is needed to regenerate the grinding tool surface. The structure number of the grinding tool is the parameter that indicates the distance between the grits, i.e., the volumetric concentration of abrasive grains in the wheel. A higher number indicates less abrasive and vice versa. For a given number, the density of the wheel, Vg (%), may be approximated as [10]:

$$V_g = 2(32 - s) \tag{1.5}$$

Since the grains are densely placed in the wheel, the assumption could be made that the distribution of the grain intervals is uniform [9, 10]. The interval can be derived from the following relation [10]:

$$\frac{\pi}{6} d^3{}_{gavg} = V_g \Delta^3 \tag{1.6}$$

Where $\triangle$ is the grain interval. The left-hand side of Eq. (3.6) indicates the volume of the grains in the grinding wheel in terms of the average grain size, and the right-hand side in terms of density.

The two sides should be equal. Therefore, from Eq. (3.6), the grain interval (mm) can be

determined as [10]:

$$\Delta = 137.9M^{-1.43}\sqrt{\frac{\pi}{32-S}} \tag{1.7}$$

To generate the grinding wheel topography, the wheel is populated with grits using the interval determined by Eq. (3.7).The distribution of the grain protrusion heights is described by a Gaussian distribution with the mean value and standard deviation determined by Eq. (3.3) and (3.4) respectively. An example with the grit number of 180 and the structural number of 8 is shown in Figure 3.3.

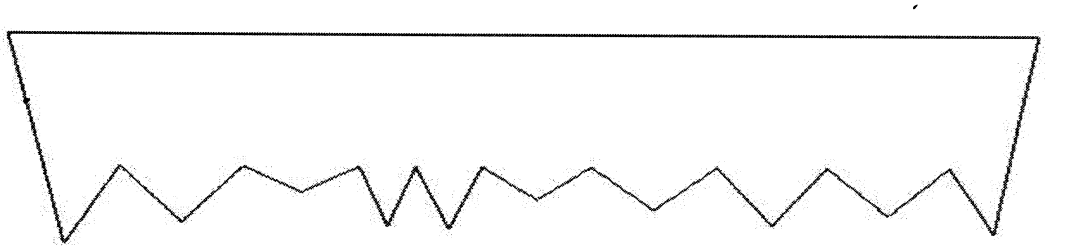

Figure 3.3: Grit section on the grinding tool surface

In order to model the grinding tool topography, the effect of all the grains must be accounted for. Each grain will cut the workpiece in the grinding process in slightly different way. In the 3D solid modelling this is realized by separating the grains into different sections, and then merging the sections together to obtain the final cut profile. Fig. 3.4 shows an example with several sections merged together. The final section is used to cut the workpiece along the path produced according to the relative movement of the grinding tool and workpiece.

Figure 3.4: The combination section of grits

The path will be discussed in the next section. For the example in Fig. 3.3, the average distance between the grits is 0.051mm. The whole tool surface is divided into 360 zones. The average number of grits can be calculated in each zone, thus, the final section can be generated by the solid modeler according to the number of grits and the distribution of the grit height and distance from each other.

3.6. Path of a single Grit

3.6.1. Reciprocal Movement

Material removal by grinding occurs mainly by a chip formation process, similar to that of other machining methods such as turning or milling. For the reciprocal face grinding shown in Fig. 3.5, the cutting path for the movement of a single grit can be resolved in two directions. The grit has a rotational speed and a feed speed. These two types of motion affect the movement of grits on the surface of the workpiece.

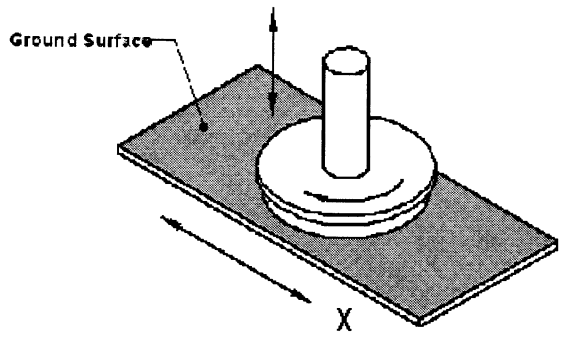

Figure 3.5: Reciprocal face grinding [1]

The x coordinate of the grit path can be determined by:

$$X = r * \sin(V_\theta * t) + V_s * t \tag{1.8}$$

Where r is the grit distance from the grinding tool center and t is the time from the beginning of the grit movement. V_θ is the grit rotational speed which is the same value as the wheel rotational speed and V_s is the feed speed.

The y value of the grit path can be described as:

$$Y = r * \cos(V_\theta * t) \tag{1.9}$$

Figure 3.6 shows the path of a single grit in reciprocal face grinding for wheel speed of 1800 rpm and table speed of 10cm/s. Fig.3.7 shows the path of a single grit with the feed speed of 2.12m/s and wheel speed of 1800 rpm.

These figures show the path of a single grit. The path will change for different grits on the wheel. Since different grits on the same radius keep the same distance during the grinding

process, the path of the grits that are located at the middle point of the wheel surface can be used as the path of the whole grit section.

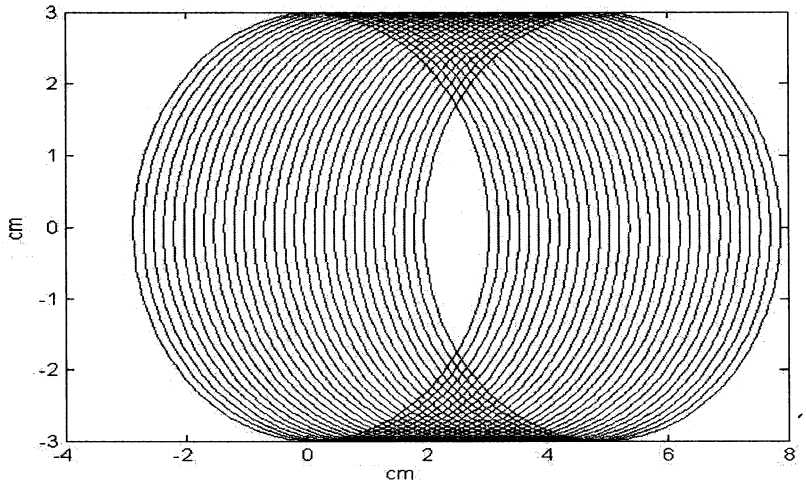

Figure 3.6: Path of a single grit in reciprocal face grinding: Vs = 10 cm/s, Vθ = 1800 rpm, r =3 cm

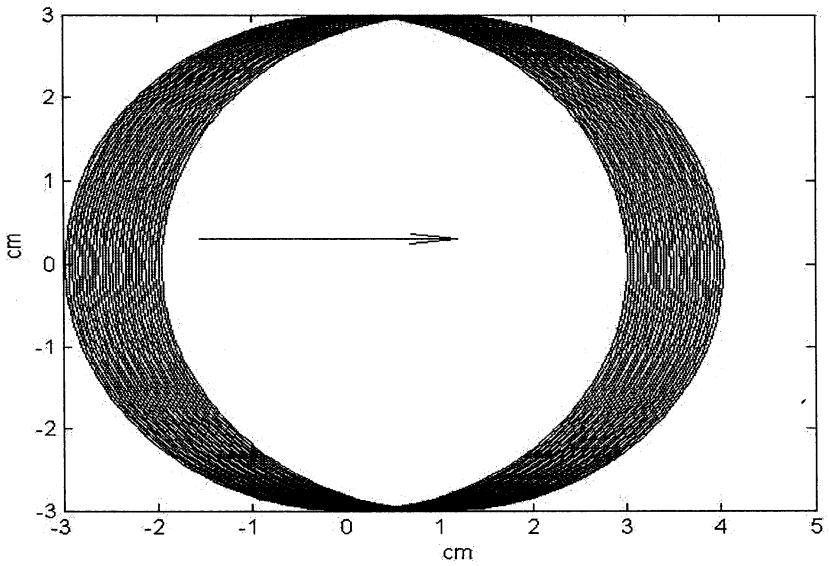

Figure 3.7: Path of a single grit in the reciprocal face grinding: Vs = 2.12cm/s, Vθ = 1800 rpm, r = 3 cm.

3.6.2. Spiral Movement

The quality of the surface is one of the most important factors that have to be considered during the grinding process. Another practical factor is the efficiency of the process. In order to balance these two factors, different grinding paths can be considered. A spiral path has been used in some applications including the polishing of silicon wafers.

When a single grit moves along a spiral, instead of a straight line, it will rotate and move along the spiral at the same time. The x coordinate of the grinding tool center during the spiral movement can be described as:

$$X = a * t * \cos(t) \tag{3.10}$$

Where t is the time and a is the constant which determines the spacing of the spiral.

The Y value of the grinding tool center during the movement can be written as:

$$Y = a * t * \sin(t) \tag{3.11}$$

Fig.3.8 shows the path of the grinding tool center. At the same time the grits will rotate along the axis of the grinding wheel. The final grit path can be obtained by combining these two movements together. For the specified grit point the x value of the grit path is expressed as:

$$X = r * \sin(V_\theta * t) + a * t * \cos(t) \tag{3.12}$$

And the y value of the grit path can be written as:

$$Y = r * \cos(V_\theta * t) + a * t * \sin(t) \tag{3.13}$$

Where r is the distance from the location of the grit to the tool center; t is the time from the

beginning of the grit movement; Vθ is the wheel rotation speed. And a is a constant. For a grit located at 4.45cm from the wheel center and the wheel speed of 1800rpm, the path of a single grit is shown in Fig. 3.9.

3.7. Modelling of Chip Removal

In grinding using the surface of the grinding tool, each grain rotates along the wheel center and moves following a complicated path, and the grooves cut in the surface of the workpiece can be modeled using the sweep function of a solid modeler. A cutting cross section of the grains is generated according to the random distribution of the grains. Once the cutting cross sections of the grains are generated, these cross sections can be used to sweep the workpiece according to the grain path to generate the cutting grooves. All the sections on the grinding wheel are combined together to obtain a final cutting section. The final cutting section engraves the workpiece along the path of the grits to generate the cutting grooves. Fig.3.10 shows the process for a single cutting cross section in reciprocal grinding. This process is

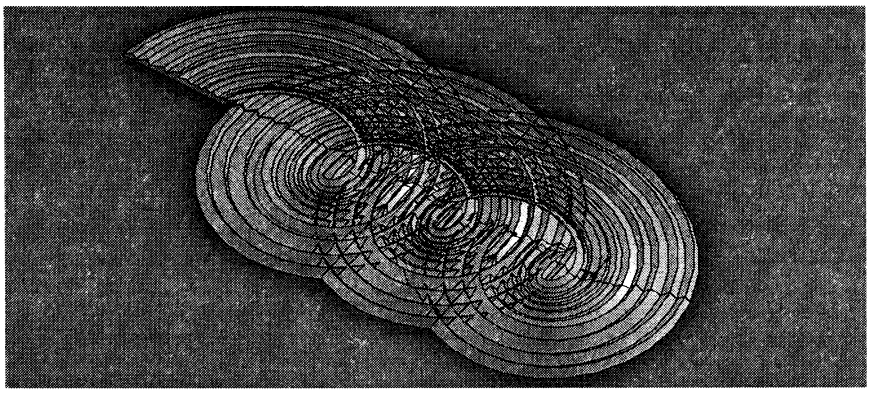

Figure 3.8: Example of chips volume

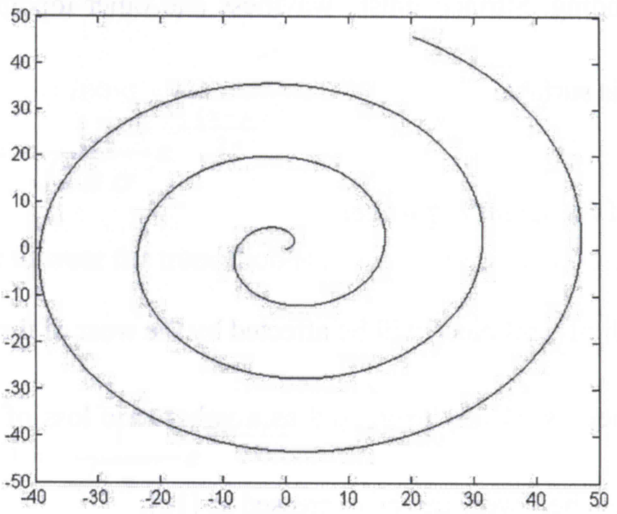

Figure 3.9: Path of grinding tool center along the spiral: a = 1.2 cm.

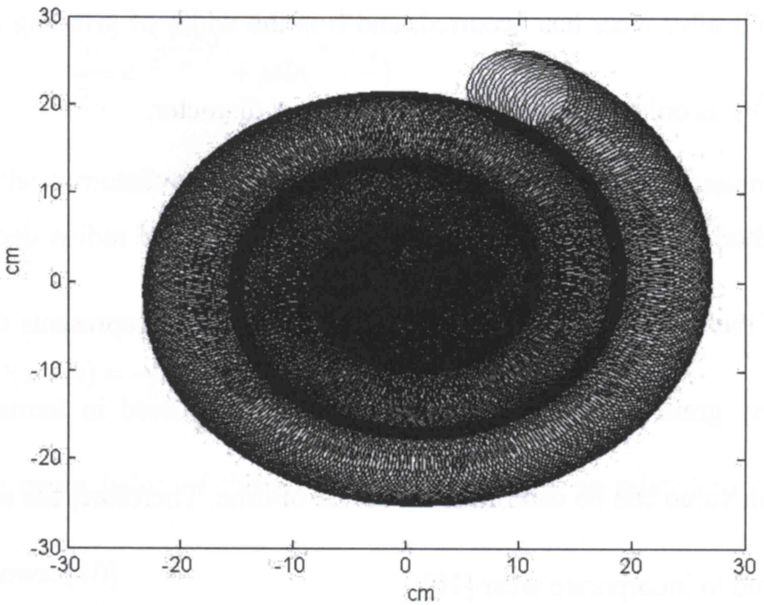

Figure 3.10: Path of grits on the outside of grinding tool along the spiral: a = 1.2 cm.

repeated until the whole surface is covered. The result is the three-dimensional model of the surface after grinding. Surface finish, waviness and other topographic information can be obtained from this surface.

3.8. Wear of the Grinding wheel

The surface finish of workpiece will be affected by the wear of the grinding wheel. The wear of a grinding wheel is usually expressed as a volumetric loss of material. The quantitative description of the wheel wear can be expressed as [10]:

$$V_w = \pi * d_s * \Delta r_s * b \qquad (3.14)$$

Where Δr_s is the measured decreased wheel radius, d_s is the mean of the wheel diameters before and after wear has occurred, and b is the width of grinding zone. In most practical cases, Δr_s is only a small fraction of the wheel diameter.

The method used to consider wear is to relate the wheel radius decrease to the truncation value of the Gaussian distribution. The truncation value represents the fracture wear of the protruding grains. Since the volumetric loss is expressed in terms of grinding time, the truncation value can be determined in terms of time. Therefore, the active cutting grains can be updated to incorporate wear [10].

Mathematically, the original protrusion height density function has a Gaussian distribution: [23]

$$f = \frac{1}{\sqrt{2\pi}\sigma} e^{-\frac{(x-\mu)^2}{2\sigma^2}} \tag{3.15}$$

Assuming that due to wear the truncation is at z, the truncated Gaussian PDF is expressed as follows: [10]:

$$f(z) = \frac{1}{\sqrt{2\pi}\sigma} e^{-\frac{(z-\mu)^2}{2\sigma^2}} \tag{3.16}$$

The mean value of the protrusion heights for the truncated distribution can be written as:

$$\mu_w = \int_{-\infty}^{z} z \frac{1}{\sqrt{2\pi}\sigma} e^{\frac{(z-\mu)^2}{2\sigma^2}} dz \tag{3.17}$$

It can be shown through mathematical manipulation that Eq. (3.17) yields [24]:

$$\mu_w = -\frac{\sigma}{\sqrt{2\pi}} e^{\frac{1}{2}(\frac{z-\mu}{\sigma})^2} + \mu\Phi(\frac{z-u}{\sigma}) \tag{3.18}$$

Where $\Phi(\cdot)$ is the cumulative distribution function of the standard Gaussian PDF defined as [10]:

$$\Phi(z-u) = \frac{1}{\sqrt{2\pi}} \int_{-\infty}^{t} e^{\frac{(z-\mu)}{2}} dt \tag{3.19}$$

Changes in the mean value of the protrusion heights can be related to the wheel radius decrease as follows: [10]

$$\Delta r = \mu - \mu_w \tag{3-20}$$

Once the wheel radius decrease is determined by Eq. (3.14) for a given volumetric loss, the

truncation value z can be numerically determined by using Eq. (3.16) to Eq. (3.20). For example, if the grit size of the grinding tool was 180, structure number was 8 and the truncation value was at 2σ, the mean value of the protrusion heights for the truncated distribution would be 36.83 μm.

Chapter 4. Case Studies

4.1. Introduction

The modelling methodology introduced in Chapter 3 was used for predictive modelling of surface finish for a number of case studies. A variety of cutting paths were examined to show the flexibility of the proposed methodology.

The grinding tool used was a wheel with the grit size 180 and structure number 8 under the condition of dry grinding. The other parameters representing the relative movements were: wheel speed of 1800rpm, wheel diameter of 88.9mm and wheel width of 28.6mm. The depth of the cut was 0.015mm and was kept constant for all the case studies. The case studies are separated into two groups according to the status of the grains: sharp and worn. In each case, the center-line average value of surface roughness (Ra) is calculated under different conditions.

4.2. Assumptions

The following assumptions were made:

- The vibration of the grinding wheel is negligible.
- The elastic-plastic deformation of cutting grains is negligible; the material of the workpiece engaged with cutting edge is totally removed out of the workpiece.

- No slide flow, built-up-edge phenomena
- Thermal effects are considered to be negligible.

4.3. Case Study I: Reciprocal Face Grinding with Sharp Grits

There are many different face grinding methods used in manufacturing industry. The first case study in this thesis is the reciprocal face grinding with sharp grits shown in Fig.4.1. The grit size of the grinding tool is 180 and its structure number is 8. The cutting parameters are listed in Table 4.1.

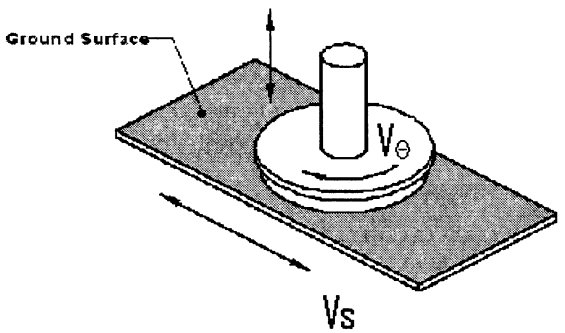

Figure 4.1: Reciprocal face grinding

Table 4.1 Parameters of the grinding tool

Symbol	V_θ	V_s	D	W
Value	1800 rpm	2.12cm/s	8.89cm	2.86cm

Where V_θ is the wheel speed, V_s represents the workpiece speed, D is the wheel diameter and W is width of the grinding surface.

The main factor that affects the grinding path in this case is the ratio of the wheel speed and workpiece speed. It will directly affect the surface roughness of the workpiece. The bigger the ratio, the better the surface finish. The parameters for the description of grit path were discussed in chapter 3. An example of the grit path in reciprocal grinding is shown in Fig.4.2.

The grit distribution and grit spacing were discussed in chapter 3. Fig.4.3 shows the profile of one cross section of the grits on the same radius.

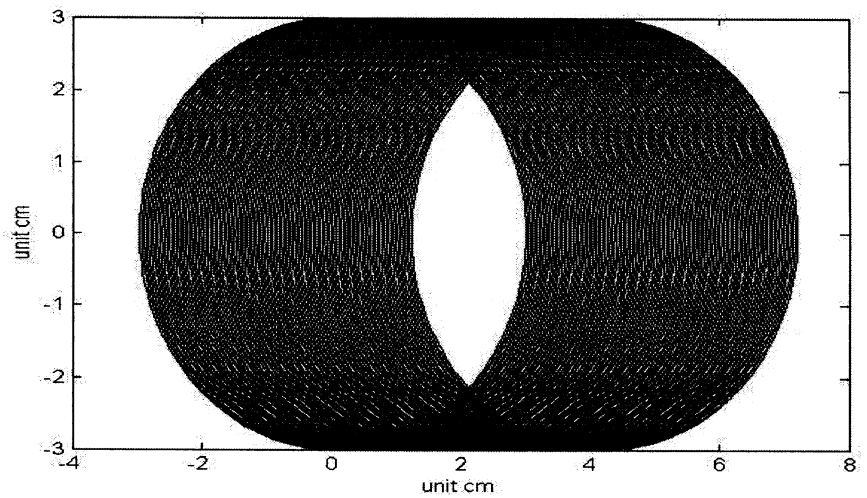

Figure 4.2: Grit path for: V_θ = 1800 rpm, V_s = 2.12 cm/s, r = 3 cm

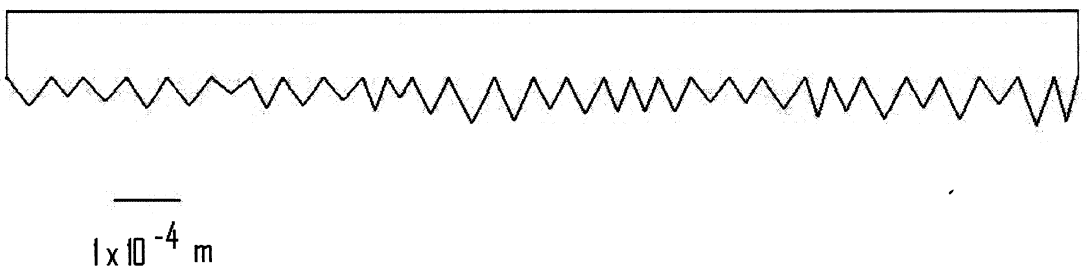

Figure 4.3: One section of grits on the same radius

The effect of multiple sections can be obtained by merging all the cutting sections together. Fig. 4.4 shows an example of such a merged section. These merged cutting cross sections will be swept along the grit path to model the cutting action of the grits.

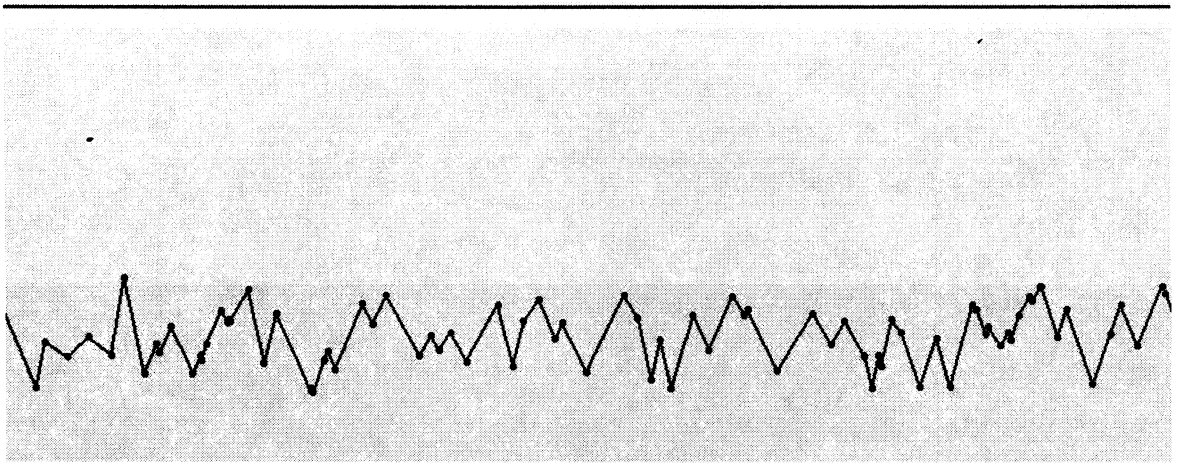

Figure 4.4: Merged cutting section

Once the grinding tool rotates one whole turn, the surface is generated which represents the cutting effect of all effective grits on the workpiece. An example of a modeled ground surface is shown in Fig.4.5. Note that the surface shows the characteristic tool marks of a ground surface.

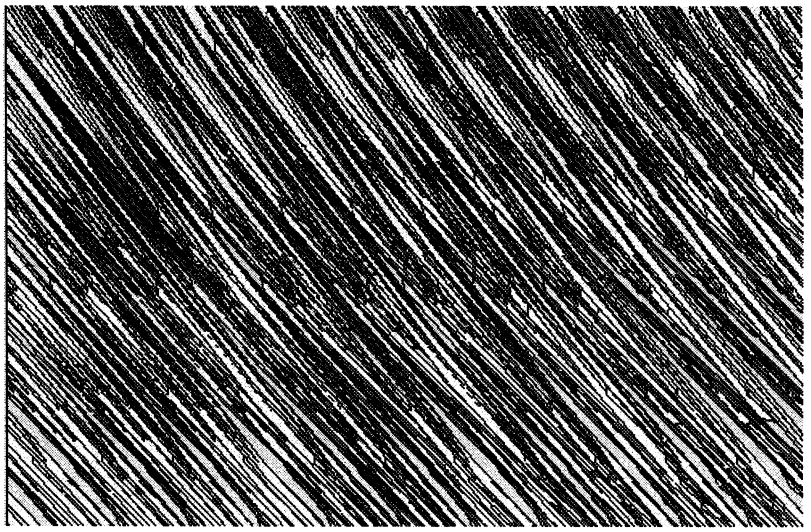

Figure 4.5: Final workpiece surface: normal grits move along the straight line

Since the modelling methodology presented here leaves a three-dimensionally sculpted surface, this surface can be directly examined to calculate surface characteristics such as surface finish of the workpiece.

In order to calculate the surface roughness, the surface was cut by a plane and the section was saved as an IGES file. The result was then retrieved from the IGES file to calculate the surface roughness. A length of 2mm was divided into 8 sections. Each section contained 60000 points which was used to calculate the surface roughness according to Eq. (4-1).

$$R_a = \frac{1}{N}\sum_{1}^{N} | z_i - z_o | \qquad (4\text{-}1)$$

The average surface roughness (Ra) for this case study was 0.312 micron.

4.4. Case Study II: Reciprocal Face Grinding with a Worn Tool

The grains will become worn during the grinding process. Many factors affect the extent of wear. In this work, only gradual wear is considered. The gradual wear causes a change in the distribution of the grit protrusion height. The wear extent depends on the time the tool is used, the relative hardness of the tool and the workpiece and the coolant condition. This change in protrusion height distribution can be modeled using a truncated normal distribution [23]. Here, we set the wear extent to be 2σ (X= σ in Fig.4.6). An example of a grit cross section after wear is shown in Fig. 4.7. The path traversed by each grit remains the same.

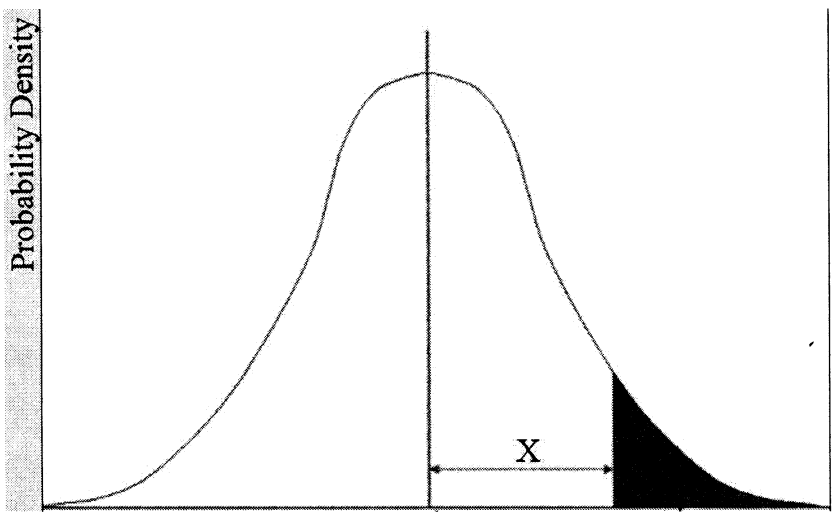

Figure 4.6: Change in protrusion height distribution caused by gradual wear

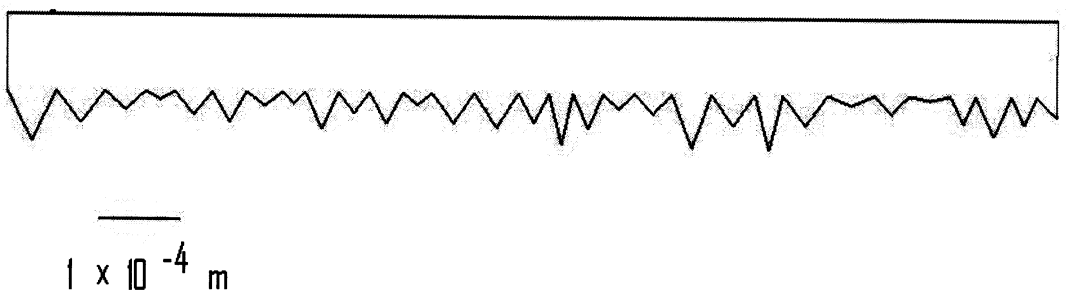

Figure 4.7: section view of worn grits

Fig. 4.8 shows the cumulative cross section of multiple sections of the grinding tool. Compared with the sharp grain in Fig.4.4, it can be observed that the worn section is flatter than the sharp one.

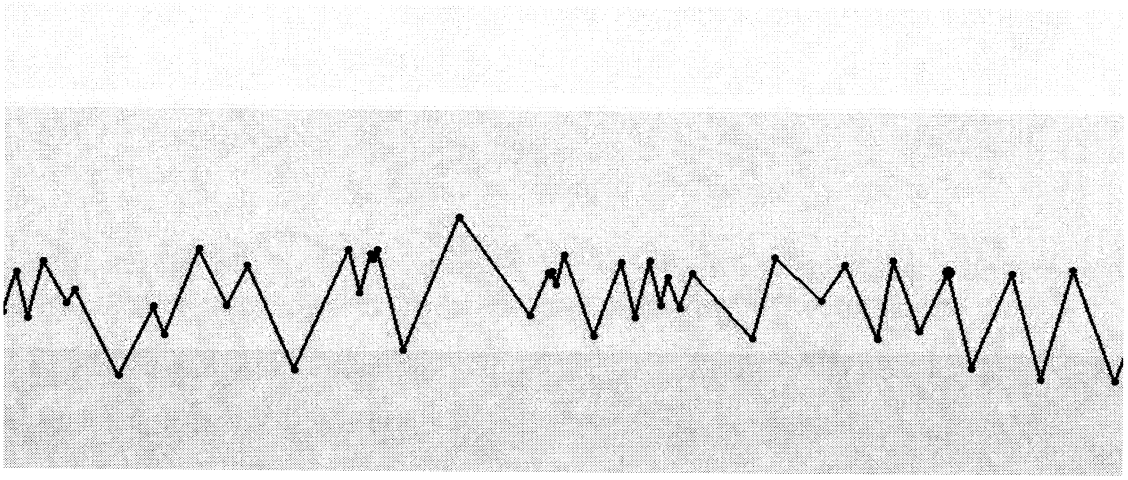

Figure 4.8: Sections views of workpiece with function of all worn grits without the movement of tool center

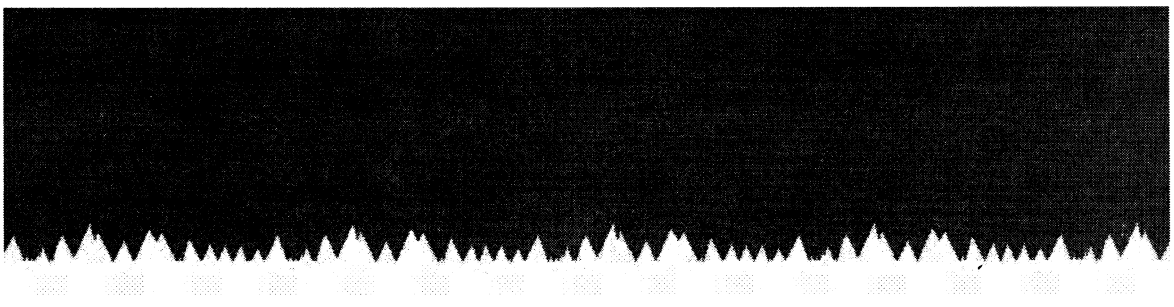

Figure 4.9: Workpiece surface section: worn grits along a straight line

After modelling the grinding action the resulting surface can be obtained. A cross section of the machined part is shown in Fig.4.9.

The average surface roughness (Ra) for this case was calculated to be 0.273 um. Although the modelling result indicates a smoother surface, in practice a worn grinding tool will generate a large amount of friction and heat. This will result in the burning of the surface and metallurgical damages. Therefore, the grinding tool should be dressed if the extent of the tool wear can cause the possibility of these damages.

4.5. Case Study III: Vertical-Spindle Spiral Surface Grinding with Sharp Grits

The third case discussed in this thesis is that of a grinding tool cutting the workpiece in a spiral pattern (Fig. 4.10). The tool parameters are the same as those in Table 4.1. The parameters for the spiral movement are listed in Table 4.2.

Table 4.2 Parameters of the grinding tool

Symbol	V_θ	a	r
Value	1800 rpm	1.2 cm	3 cm

Where V_θ is the wheel speed, *a* represents the constant which dominates the spacing of the spiral, r is the distance from the center of the grinding tool to the center of the wheel surface along the radius.

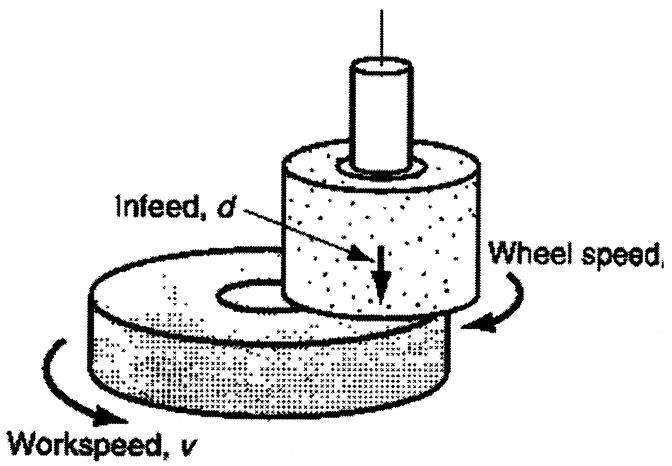

Figure 4.10: Grinding with a spiral cutting path

During the grinding process, grits will rotate along the wheel and follow the spiral as well. The final path is the combination of the two movements. The final path of the section grits along the spiral is shown in Fig. 4.11 with the all the parameters.

The cutting groves generated by the grains are shown in Fig.4.12. The resulting surface roughness was calculated as described in previous sections. The average roughness in this case was Ra 0.305 micron.

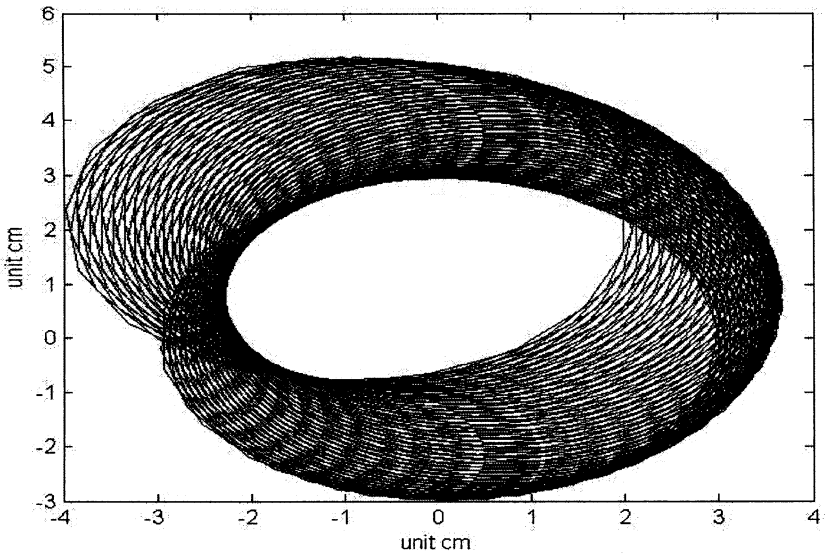

Figure 4.11: Path of a single grit in spiral cutting

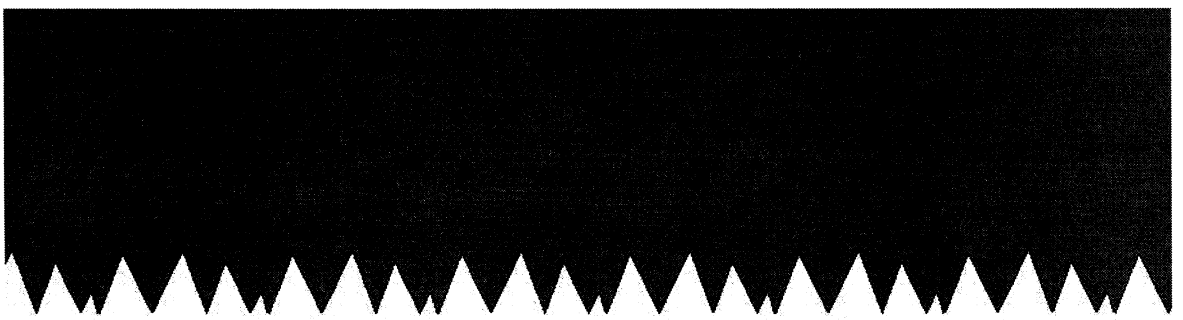

Figure 4.12: Final workpiece surface section: normal grits move along a spiral

4.6. Case Study IV: Vertical-Spindle Spiral Path Surface Grinding with a Worn Tool

Grinding on a spiral path with a worn tool was performed in this case study. Again a truncated normal distribution was used to model the effect of gradual wear. The same cutting path was used as before. The result in this case is shown in Fig.4.13. The resulting surface roughness was 0.257 micron.

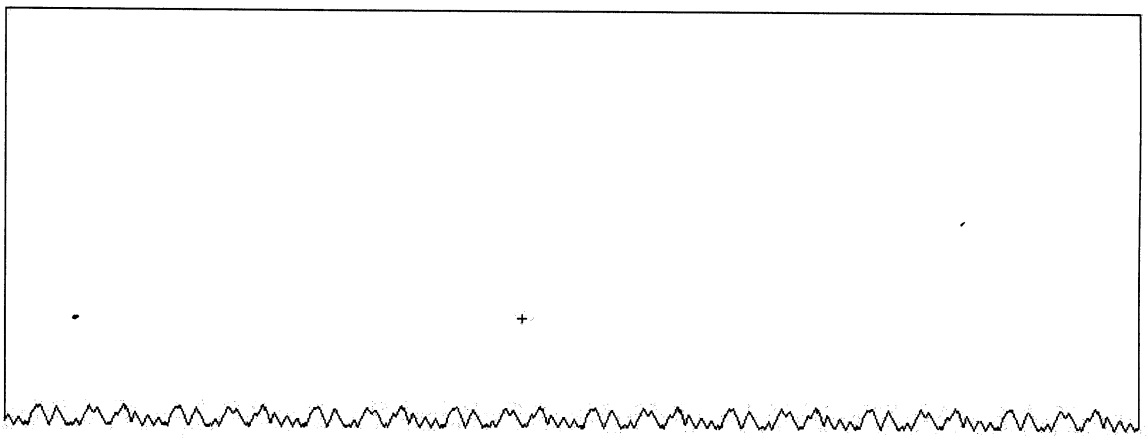

Figure 4.13: Workpiece surface: worn grits along a spiral path

4.7. Case Study V: Grinding of Wire-Sawn Silicon Wafers

The proposed methodology can be used for modelling grinding operations with a complex tool path. An example is the grinding of wire-sawn silicon wafers [16] (see Fig. 2.6 repeated here as Fig. 4.14).

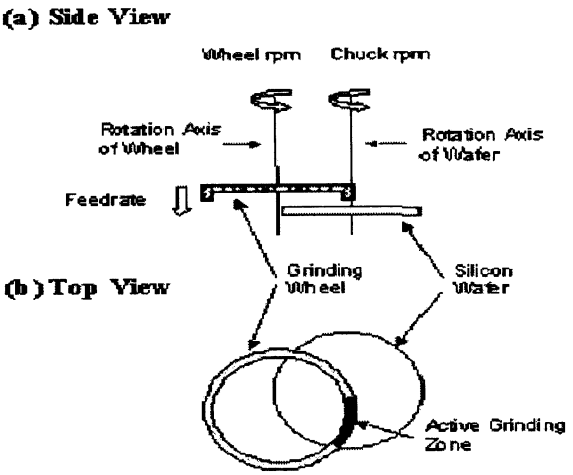

Figure 4.14: Illustration of wafer grinding [16]

The combination of two rotary motions in this case creates a complex tool path which is very difficult to model using conventional methods. Using the proposed methodology, first a cross section of the cutting grit was generated using the grinding wheel parameters of grit size 180 and structure number equal to 8. The path of each grit was then generated by combining the two rotary motions. In this case, the grinding wheel was rotating at 1800 rpm and the silicon wafer was rotating at 300 rpm. This process was repeated until the whole surface was covered. Fig. 4.15 shows a cross section through the surface and Fig. 4.16 shows the surface after grinding. The average surface roughness was calculated to be 0.07 micron.

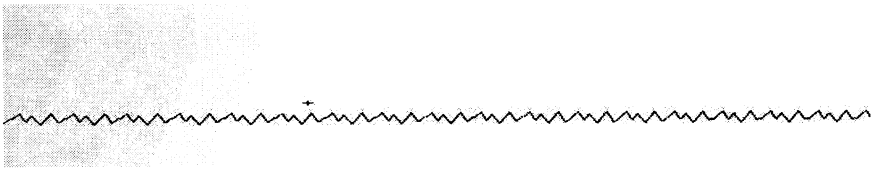

Figure 4.15: A cross section through silicon wafer

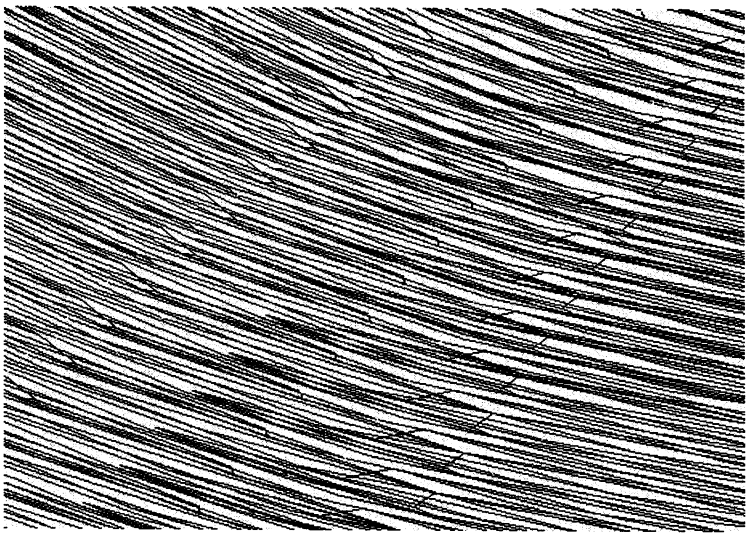

Figure 4.16: Surface of silicon wafer after grinding

4.8. **Results Summary**

Table4.3 shows the results for the different case studies.

Table 4.3 Results for different case studies

Case	Reciprocal Grinding		Sprial Grinding		Wafer grinding
	Sharp grits	Wear grits	Sharp grits	Wear grits	Sharp grits
Ra	0.312 μm	0.273 μm	0.305 μm	0.257 μm	0.07 μm

Chapter 5. Discussion

5.1. Comparison with Literature

The goal of this work was to introduce a novel predictive modelling methodology for grinding processes with complex tool path. This methodology fills a gap in the literature by using advances in solid modelling technology and widely available commercial solid modelers. The results for the case studies are consistent with surface finish measurement reported in literature under similar conditions [9]. That means this modelling can be used to simulate the grinding process.

5.2. Discussion

The modelling method developed in this thesis makes it easy to predict the effectiveness of different grinding strategies. For example, the results with the straight line path are not as good as those with the spiral path. The reason is that, during the spiral movement, the grits have more overlapping cutting action. On the contrary, the grits repeat the same path in the process of the straight line grinding, and, therefore, is not as efficient. The three dimensional modelling presented here can also be used for designing grinding processes which have to generate surfaces with strict specifications not only on surface roughness but also waviness and lay. This capability does not exist with modelling techniques reported in the literature.

The modelling results under the wear condition were better than those with the sharp grit. This reflects the fact that factors such as plastic deformation and plowing were not considered in the model. In practice, however, a grinding tool either self sharpens or is dressed regularly to avoid workpiece damage. Therefore, the model can still be used to devise effective cutting paths for sharp tools.

Chapter 6. Conclusions and Future Work

6.1. Conclusions

A novel predictive modelling methodology was introduced. The method uses commercial solid modelers to represent the cutting action of abrasive grits in a grinding process. The proposed methodology is specially suited to grinding processes which generate a complicated cutting path.

6.2. Contributions

The contributions of this thesis include:

A novel three-dimensional modelling methodology has been developed to predict the surface characteristics of ground surfaces. The methodology does not require time consuming iterations or searches.

The modelling method can easily be applied to any complex grinding operations. This makes it possible to study the effect of different tool path designs.

6.3. Future Work

Vibration, external and self generated, can affect the quality of the surfaces generated by the grinding process. The modelling methodology described in this thesis can be improved by including the effect of vibration. Since vibration is basically a relative motion between the

tool and workpiece, it could be included as a superimposed motion during the chip removal process. This will require more elaborate programming and the use of specially written software.

References

1. Mikell P.Groover, Fundaments of modern manufacturing, Prentice Hall (1996).
2. M.C. Show, Principle of abrasive processing, Oxford University Press (1996).
3. H. Saglam, F. Unsacar and S. Yaldiz, An experimental investigation as to the effect of cutting parameters on roundness error and surface roughness in cylindrical grinding, *International Journal of Production Research*, Vol. 43, No. 11, 1 (2005).
4. J. Kopac and P. Krajnik, High-performance grinding—A review, *Journal of Materials Processing Technology,* Vol. 175, 278–284 (2006).
5. P. Asokan N. Baskarl, K. Babu, G. Prabhaharan and R. Saravanan, Optimization of Surface Grinding Operations Using Particle Swarm Optimization Technique, *Journal of Manufacturing Science and Engineering*, Vol. 127, 891 (2005).
6. I. Inasaki, Grinding process simulation based on the wheel topography measurement, *Annals of CIRP,* Vol. 54 (1), 347-350 (1996).
7. T. Suto and T. Sata, Simulation of grinding process based on wheel surface characteristics, *Bulletin of Japan Society of Precision Engineering*, Vol. 15 (1), 27–33 (1981).
8. X. Chen and W.B. Rome, Analysis and simulation of the grinding process. Part I: generation of the grinding wheel surface, *International Journal of Machine tools and manufacture*, Vol. 36 (8), 871-882 (1996).

9. S. Agarwal and P. Venkateswara Yao, A new surface roughness prediction model for ceramic grinding, *Journal of Engineering Manufacture*, Vol. 219, 811 – 819 (2005).

10. X. Zhou and F. Xi, Modelling and predicting surface roughness of the grinding process, *International Journal of machine tools & Manufacture*, Vol. 42, 969-977 (2002).

11. A.A. Torrance and J.A. Badger, The relation between the traverse dressing of vitrified grinding wheels and their performance, *International Journal of Machine Tools and Manufacture*, Vol. 40 (12), 1787-1811 (2000).

12. T.A. Nyugen and D.L.Butler Simulation of surface grinding Process, Part 2: interaction of the abrasive grain with the workpiece, *International Journal of Machine Tools & Manufacture*, Vol. 45, 1329-1336 (2005).

13. L. Hecker Regelio and Y. Liang, Predictive modelling of surface roughness in grinding, *International Journal of Machine Tools & Manufacture*, Vol. 43, 755-761 (2003).

14. Hongqi Li and C. Shin Yung, A Time-Domain Dynamic Model for Chatter Prediction of Cylindrical Plunge Grinding Processes, *ASME*, Vol. 128, (2006).

15. S. Samhouri Murad and W. Surgenor Brian, Surface roughness in grinding: on-line prediction with adaptive neuro-fuzzy inference system, *Journal of Manufac- turing Science and Engineering*, Transactions of NAMRI/SME 58 Vol. 33 (2005).

16. Yue Jiao1, et al., A Fuzzy Adaptive Network Model for Waviness Removal in

Grinding of Wire-Sawn Silicon Wafers, *Journal of Manufacturing Science and Engineering*, Vol. 128, 938-943 (2006).

17. A. Doman, A. Warkentin and R. Bauer, A survey of recent grinding wheel topography models, *International Journal of Machine Tools & Manufacture*, Vol.46, 343–352 (2006).

18. S. Malkin, Grinding Technology Theory and Applications of Machining with Abrasives, Ellis Horwood Edition (2007).

19. J. Verkerk, Final Report concerning CIRP Cooperative Work in the Characterization of Grinding Wheel Topography, *Annals of the CIPR*, Vol. 26, 385-395 (1977).

20. S. Tooe, K. Umino and N. Shinozaki, Study on Grinding Characteristic of Grinding Wheel, *Japan Society of Precision Engineering*, Vol. 21(4) (1987).

21. X. Zhou, Modeling and Predicting Surface Roughness of the Grinding Process, Thesis for Master of Engineering Science, University of Western Ontario (2001).

22. Philip Koshy, Lewis K. Ives and Said Jahanmir, Simulation of diamond-ground surfaces, *International Journal of Machine Tools & Manufacture*, Vol. 39, 1451–1470 (1999).

23. A. Hald, Statistical theory with engineering applications, John Wiley & Sons, Inc. (1952).

24. X. Chen, and W.B.Rowe, Analysis and simulation based on the wheel topography measurement, *Annals of the CIRP*, Vol. 45, 347-350 (1996).